Heat Generation and Radiation Effects on Steady MHD Free Convection Flow of Micropolar Fluid Past a Moving Surface

M. Gnaneswara Reddy

Dept. of Mathematics, Acharya Nagarjuna University Ongole Campus, Ongole - 523 001 (INDIA)

E-Mail: mgrmaths@gmail.com

ABSTRACT

In this paper, the study of heat generation and radiation effects of magnetohydrodynamic free convection flow of a micropolar fluid past a continuously moving surface heat generation has been investigated. Using the similarity transformations, the governing equations have been transformed into a system of ordinary differential equations. These differential equations are highly nonlinear which cannot be solved analytically. Therefore, finite element method has been used for solving it. The effect of various important parameters on the velocity, microrotation and temperature functions has been extensively investigated. Results for velocity, microrotation and temperature functions are shown graphically. The skin friction and the rate of heat transfer have also been computed and are presented through tables.

Key words: Free Convection, MHD, Radiation, Heat generation

1. INTRODUCTION

Micropolar fluids are referred to those fluids that contain micro-constituents that can undergo rotation which affect the hydrodynamics of the flow. In this context, they can be distinctly non-Newtonian in nature. The basic continuum theory for this class of fluids was originally formulated by Eringen [1]. The equations governing the flow of a micropolar fluid involve a microrotation vector and a gyration parameter in addition to the classical velocity vector field. Eringen's micropolar fluid theory has been employed to study a number of various flow situations such as the flow of low concentration suspensions, liquid crystals, blood, and turbulent shear flows. The theory may also be applied to explain the flow of colloidal solutions, fluids with additives and many other situations.

The flow and heat transfer from a continuous surface in a parallel free stream of micropolar fluid is studied by Gorla et al. [2]. The effect of radiation on heat transfer over a stretching surface is important in the context of space technology and processes involving high temperature. Raptis [3] studied the flow of a micropolar fluid past a continuously moving plate by the presence of radiation. El-Arabawy [4] analyzed the problem of the effect of suction/injection on the flow of a micropolar fluid past a continuously moving plate in the presence of radiation. Recently, Seddeek et al. [5]

investigated the analytical solution for the effect of radiation on flow of a magneto-micropolar fluid past a continuously moving plate with suction and blowing.

In certain applications such as those involving heat removal from nuclear fuel debris, underground disposal of radioactive waste material, storage of food stuffs, and exothermic chemical reactions and dissociating fluids in packed-bed reactors, the working fluid heat generation or absorption effects are important.

The present paper contains an analysis of the radiation heat generation effects of magnetohydrodynamic free convection flow of a micropolar fluid past a continuously moving surface. Using the similarity transformations, the governing equations have been transformed into a set of ordinary differential equations, which are nonlinear and cannot be solved analytically, therefore, finite element method has been used for solving it. The results for velocity, microrotation and temperature functions are carried out for the wide range of important parameters. The skin friction and the rate of heat transfer have also been computed for these parameters.

2. MATHEMATICAL FORMULATION

Consider the steady, two-dimensional flow of an incompressible electrically conducting micropolar fluid past a continuously moving sheet in the presence of heat generation and thermal radiation effects. The sheet is stretched with a linear velocity $u_w = Bx$, where B is a positive constant and x - is the distance from the slit where the sheet originates. A uniform magnetic field of strength B_0 is assumed to be applied in the direction normal to the surface. The fluid is assumed to be viscous and has constant properties. The applied magnetic field is assumed to be constant and the magnetic Reynolds number is assumed to be small so that the induced magnetic field is neglected. Under the usual boundary layer approximation, the governing equations are given as follows :

Continuity equation:

$$\frac{\partial u}{\partial x}+\frac{\partial u}{\partial y}=0 \tag{1}$$

Momentum equation:

$$u\frac{\partial u}{\partial x}+v\frac{\partial u}{\partial y}=\nu\frac{\partial^2 u}{\partial y^2}+k_1\frac{\partial N}{\partial y}+g\beta\left(T-T_\infty\right)-\frac{\sigma B_0^2}{\rho}u \tag{2}$$

Angular momentum equation:

$$G_1\frac{\partial^2 N}{\partial y^2}-2N-\frac{\partial u}{\partial y}=0 \tag{3}$$

Energy equation:

$$u\frac{\partial T}{\partial x}+v\frac{\partial T}{\partial y}=\alpha\frac{\partial^2 T}{\partial y^2}-\frac{1}{\rho c_p}\frac{\partial q_r}{\partial y}+\frac{Q}{\rho c_p}Q(T-T_\infty) \tag{4}$$

subject to the boundary conditions

$$\begin{aligned} &u=Bx,\quad v=0,\ N=-\frac{1}{2}\frac{\partial u}{\partial y},\ T=T_w \quad at\ \ y=0\\ &u\to 0,\quad N\to 0,\quad T\to T_\infty \qquad as\quad y\to\infty \end{aligned} \tag{5}$$

where u, v are the velocity components in the x and y direction respectively, ρ is the density of the fluid, N is the microrotation component whose direction of rotation is in the xy plane, ν is the kinematic viscosity, G_1 is the microrotation constant B_0 - the magnetic induction, σ - the electrical conductivity of the fluid, k - the thermal conductivity, T is the temperature of the fluid in the boundary layer, T_∞ is the temperature of the fluid far away from the plate, α - the thermal diffusivity, c_p is the specific heat at constant pressure, $k_1 = s/\rho$ is the coupling constant, s is a constant characteristic of the fluid. Q is constant heat flux per unit area.

By using the Rosseland approximation Brewster (Brewster 1992), the radiative heat flux q_r is given by

$$q_r=-\frac{4\sigma_s}{3k_e}\frac{\partial T^4}{\partial y} \tag{6}$$

where σ_s is the Stefan-Boltzmann constant and k_e - the mean absorption coefficient.

It should be noted that by using the Rosseland approximation, the present analysis is limited to optically thick fluids. If the temperature differences within the flow are sufficiently small, then Equation (6) can be linearized by expanding T^4 into the Taylor series about T_∞, which after neglecting higher order terms takes the form

$$T^4 \cong 4T_\infty^{\,3}T-3T_\infty^{\,4} \tag{7}$$

In view of Equations (6) and (7), Equation (4) reduces to

$$u\frac{\partial T}{\partial x}+v\frac{\partial T}{\partial y}=\alpha\frac{\partial^2 T}{\partial y^2}+\frac{16\sigma_s\ T_\infty^{\,3}}{3k_e\rho\ c_p}\frac{\partial^2 T}{\partial y^2}+Q(T-T_\infty) \tag{8}$$

The velocity components u and v can be expressed in terms of the stream function ψ such that

$$u=\frac{\partial\psi}{\partial y}\ \text{and}\ v=-\frac{\partial\psi}{\partial x}$$

It may be verified that the continuity equation is automatically satisfied. Introducing the following non-dimensional variables.

$$\eta=\left(\frac{B}{\nu}\right)^{1/2} y,\quad \psi=(B\nu)^{1/2} xf(\eta),\quad N=\left(\frac{B^3}{\nu}\right)^{1/2} xg(\eta),\ \theta=\frac{T-T_\infty}{T_w-T_\infty},\ Gr=\frac{g\beta(T_w-T_\infty)}{xB^2},$$

$$M=\frac{\sigma B_0^2}{\rho B},\quad K=\frac{k_1}{\nu},\quad G=\frac{G_1}{\nu},\quad \Pr=\frac{\nu\rho c_p}{k},\quad R=\frac{3k_e k}{16\sigma_s T_\infty^3},\ \phi=\frac{2Q}{\rho c_p u_w} \tag{9}$$

In view of Equation (9), the equations (2), (3) and (8) transform into the following ordinary nonlinear system of differential equations.

$$f'''+ff''-(f')^2+Gr\,\theta-Mf'+Kg'=0 \tag{10}$$

$$Gg''-(2g+f'')=0 \tag{11}$$

$$(1+R)\theta''+R\Pr f\theta'+R\Pr\phi\theta=0 \tag{12}$$

The corresponding boundary conditions are

$$f=0,\ f'=1,\ g=-\frac{1}{2}f''(0),\quad \theta=1\quad at\quad \eta=0 \tag{13}$$

$$f'\to 0,\quad g\to 0,\quad \theta\to 0\qquad as\quad \eta\to\infty$$

where Gr is the thermal Grashof number, M - the magnetic field parameter, K - the coupling constant, G - microrotation parameter, R - radiation parameter, Pr - the Prandtl number, ϕ - the heat generation parameter.

For the type of flow under consideration, the physical quantities such as the wall shear stress, surface heat flux and the surface mass flux are very important, which are given by

$$\tau_w=\mu\left(\frac{\partial u}{\partial y}\right)_{y=0} \tag{14}$$

$$q_w=-k\left(\frac{\partial T}{\partial y}\right)_{y=0} \tag{15}$$

where μ is the viscosity and k - the thermal conductivity.

Hence, the skin-friction coefficient, Nusselt number and Sherwood number near the plate in non-dimensional form are given by

$$C_f=\frac{2\tau_w}{\rho u_w^2}=2(\mathrm{Re}_\delta)^{-1} f''(0) \tag{16}$$

$$Nu = \frac{xq_w}{k\left(T_w - T_\infty\right)} = -\theta'(0) \tag{17}$$

where $\mathrm{Re}_\delta = \frac{u_w x}{\nu}$ is the Reynolds number.

3. METHOD OF SOLUTION

The set of differential Equations (10) to (12) subject to the boundary conditions (13) are highly nonlinear, coupled and therefore it cannot be solved analytically. Hence, following Reddy (Reddy 1985) and Bathe (Bathe 1996), the finite element method is used to obtain an accurate and efficient solution to the boundary value problem under consideration. The fundamental steps comprising the method are as follows:

Step 1: Discretization of the domain into elements:

The whole domain is divided into finite number of *sub-domains*, a process known as discretization of the domain. Each sub-domain is termed a *finite element*. The collection of elements is designated the *finite element mesh*.

Step 2: Derivation of the element equations:

The derivation of finite element equations i.e. algebraic equations among the unknown parameters of the finite element approximation, involves the following three steps:

a. Construct the variational formulation of the differential equation.

b. Assume the form of the approximate solution over a typical finite element.

c. Derive the finite element equations by substituting the approximate solution into variational formulation.

Step 3: Assembly of element equations:

The algebraic equations so obtained are assembled by imposing the *inter-element* continuity conditions. This yields a large number of algebraic equations, constituting the *global finite element model*, which governs the whole flow domain.

Step 4: Impositions of boundary conditions:

The physical boundary conditions defined in equation (15) are imposed on the assembled equations.

Step 5: Solution of the assembled equations:

The final matrix equation can be solved by a direct or indirect (iterative) method. For computational purposes, the coordinate η is varied from 0 to $\eta_{\max} = 6$, where $\eta_{\max}$ represents infinity i.e. external to the momentum, energy and concentration boundary layers. The whole domain is divided into a set of 100 line elements of equal width 0.05, each element being three noded. Thus after assembly of all the elements equations we obtain a matrix of order 201×201. This system of equations as obtained after assembly of the elements equations is non-linear therefore an iterative scheme has been used to solve it. The system is linearized by incorporating known functions. After applying the given boundary conditions only a system of 195 equations remains for the solution which has been solved using Gauss elimination method. This process is repeated until the desired accuracy of 0.0005 is obtained.

4. RESULTS AND DISCUSSION

To verify the proper treatment of the problem, our numerical results have been compared for Nusselt number $-\theta'(0)$ with those obtained by Raptis [7] for various values of M. The results of this comparison are given in Table 1. The results show a good agreement.

The distribution of the velocity, microrotation and temperature functions with the variation of Grashof number, material parameter, magnetic parameter, heat generation parameter and radiation parameter has been shown graphically in Figures 1-14. In the present study we adopted the following default parameter values of finite element computations $Gr = 1.0$, $K = 1.0$, $G = 1.0$, $M = 1.0$, $R = 1.0$, $\phi = 1.0$, and $\Pr = 0.71$. All graphs therefore correspond to these values unless specifically indicated on the appropriate graph.

Fig. 1 displays the results for the velocity distribution for various values of Gr. It is seen that velocity increases with the increase in, G*r* thereby, increasing the boundary layer. Fig. 2 shows the microrotation distribution with the variation of. G*r* Microrotation decreases with the increase in G*r* and creating a reverse rotation only near the boundary for large values of G*r*. Fig. 3 depicts the temperature distribution which decreases with the increase in G*r*. It is observed that the cooling of fluid takes place within the boundary layer.

Figure 4 shows the resulting dimensionless velocity profiles $f'(r_1)$ for various values of the material parameter K. It is observed that the velocity boundary layer thickness increases with increasing values of K associated with a decrease in the wall velocity gradient. Figure 5 shows the microrotation distribution with the variation of material parameter K. The microrotation increases with increase in K.

Figure 7 illustrates the velocity profile for different values of the magnetic parameter M. It shows that for opposing flow the velocity decreases with the increase in M. It is demonstrated from the Figure 7 that the microrotation increases with the increase of M. Figure 8 represents the temperature distribution with the variation of magnetic parameter. It increases with increase in magnetic parameter for the flow. Thus the high temperature can be controlled by magnetic parameter M, which is required in many engineering applications.

Figures 9, 10 and 11 represents the effect of radiation parameter R on the velocity, microrotation and temperature functions, respectively. It is clear from the figures that the velocity and temperature decrease with an increase in R, while microrotation increases with an increase in R.

Fig. 12 shows the effect of the heat generation parameter ϕ on f '. It is observed that f ' increases as the heat generation parameter ϕ increases. The effect of the heat generation parameter ϕ on g within the boundary layer region is observed in Fig. 13. It is apparent from this figure that g increases as the heat generation parameter (ϕ>0) decreases. Fig. 14 displays the effect of the heat generation parameter ϕ on θ. It is shown that as the heat generation parameter Ø increases the thermal boundary layer thickness increases.

The skin-friction coefficient f''(0) and the Nusselt number $-\theta'(0)$ for different values of Gr, K, M,R and ϕ and are tabulated in Table 2. It is obvious from the table that the skin-friction coefficient numerically increases with an increase in and, while decreases with an increase in Gr, ϕ and R. The rate of heat transfer increases with the increase in m and k Gr, ϕ and R while decreases with an increase in K and M.

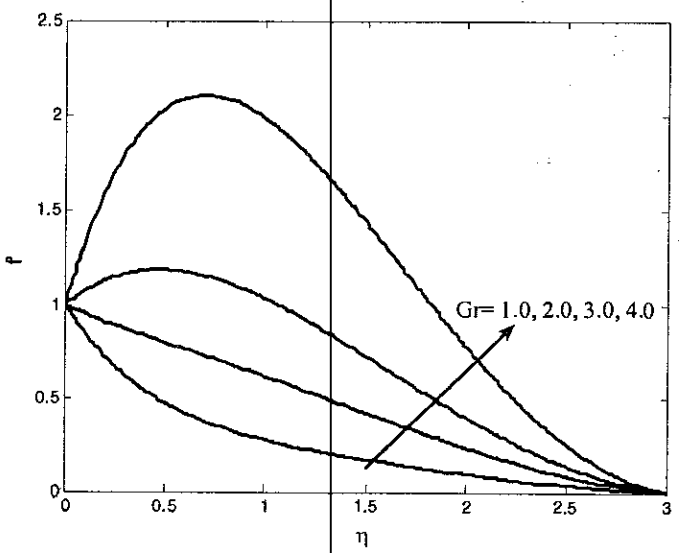

Figure 1: Velocity distribution for different Gr

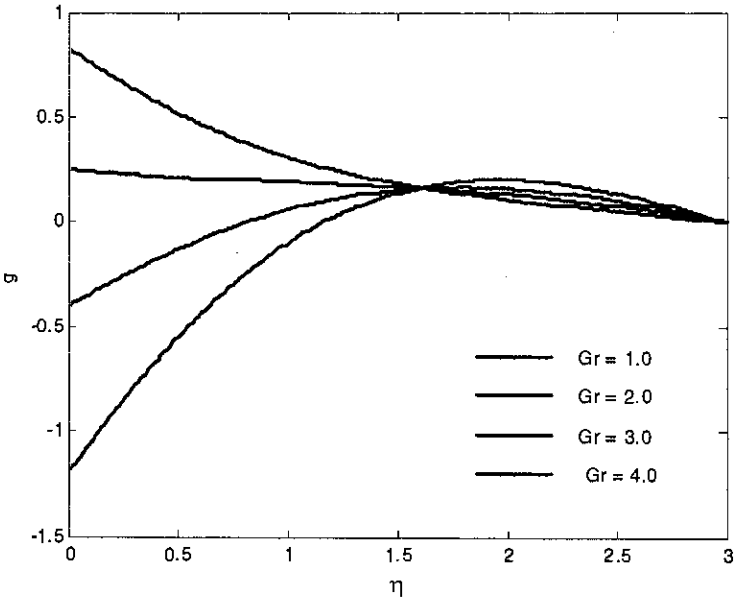

Figure 2: Microrotation distribution for different Gr

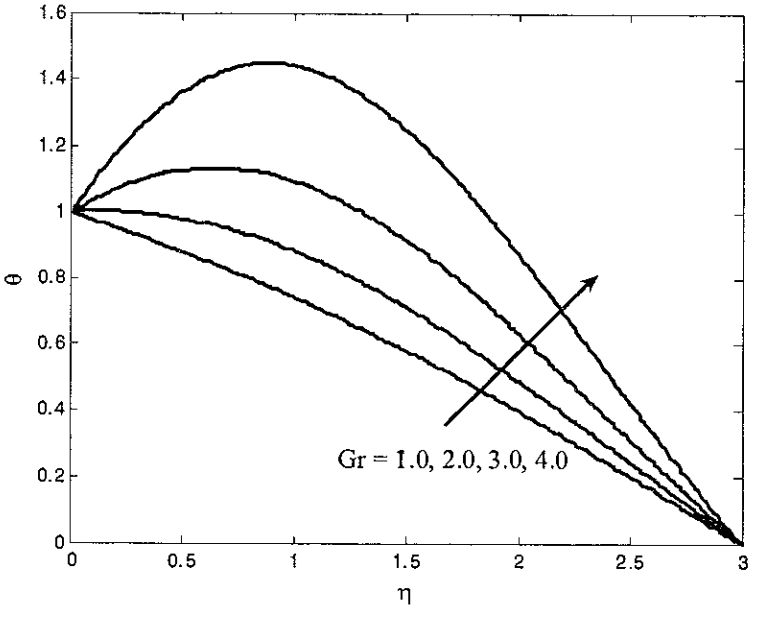

Figure 3: Temperature distribution for different Gr

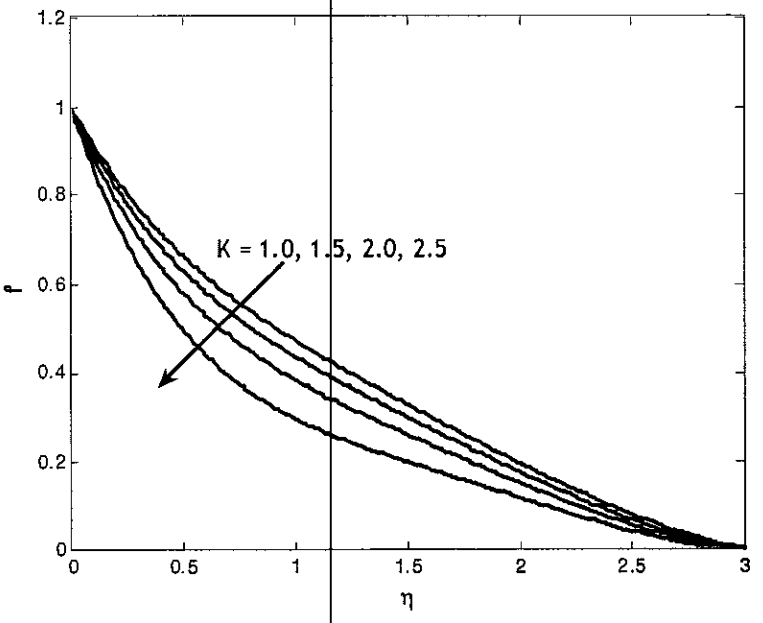

Figure 4: Velocity distribution for different K

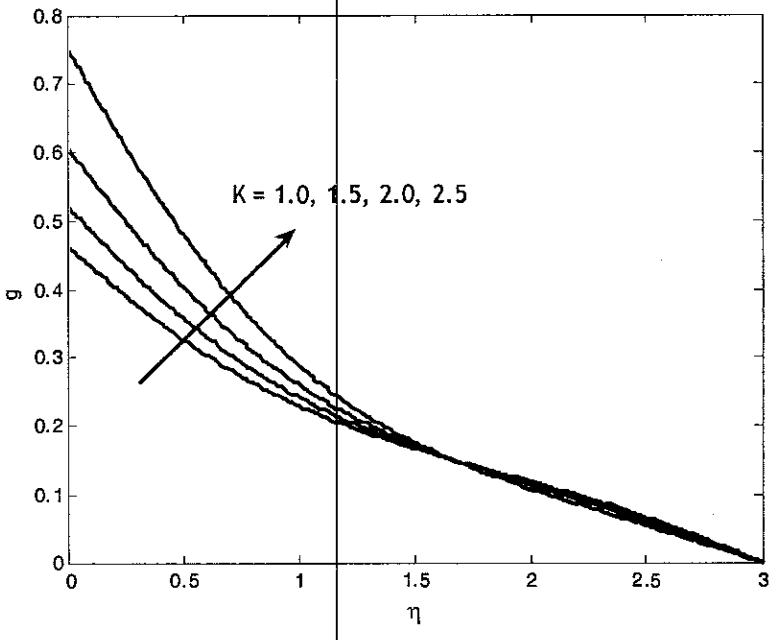

Figure 5: Microrotation distribution for different K

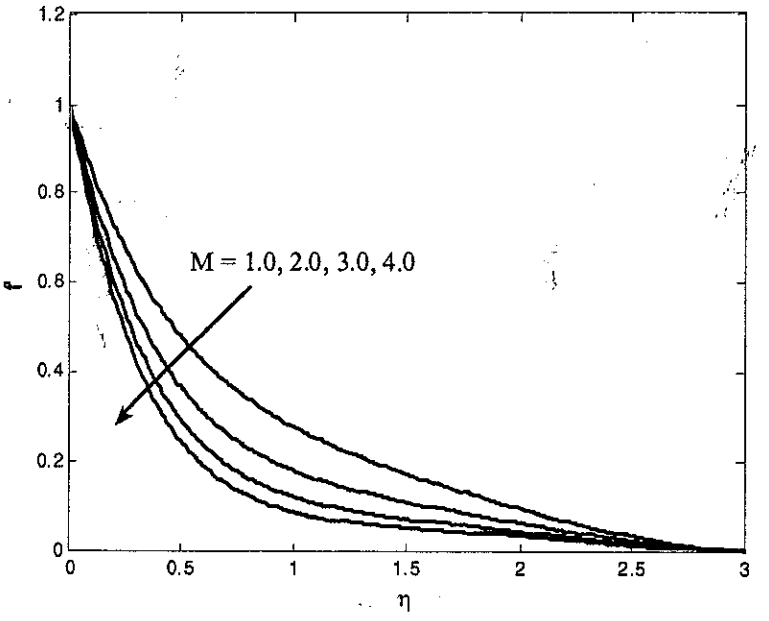

Figure 6: Velocity distribution for different M

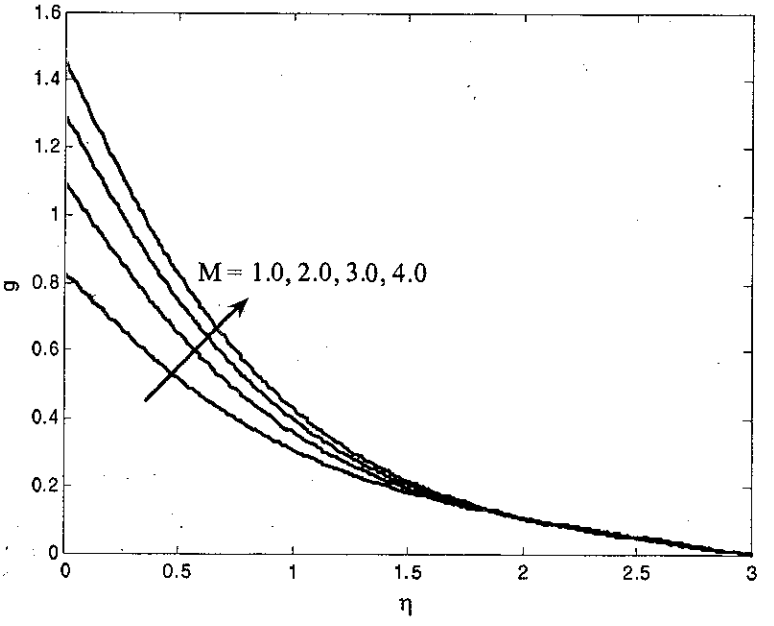

Figure 7: Microrotation distribution for different M

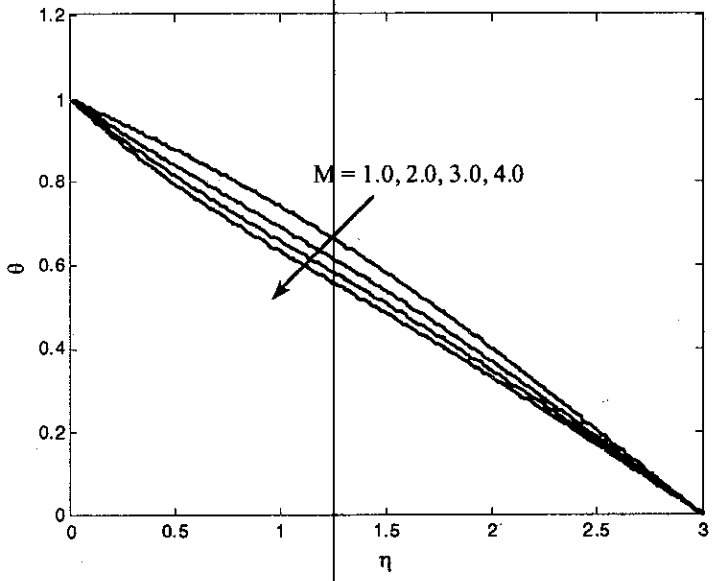

Figure 8: Temperature distribution for different M

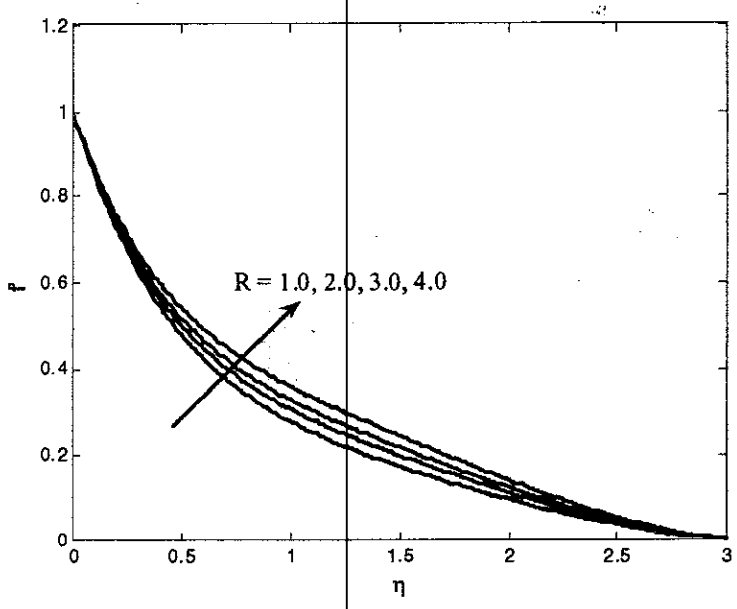

Figure 9: Velocity distribution for different R

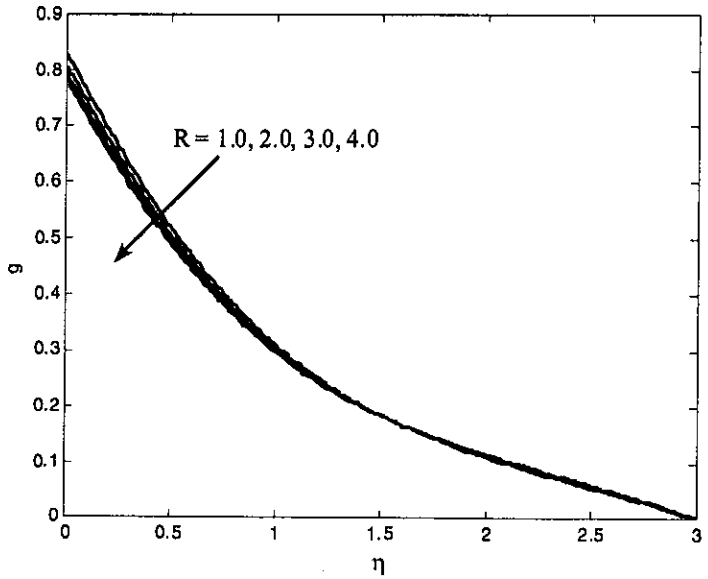

Figure 10: Microrotation distribution for different R

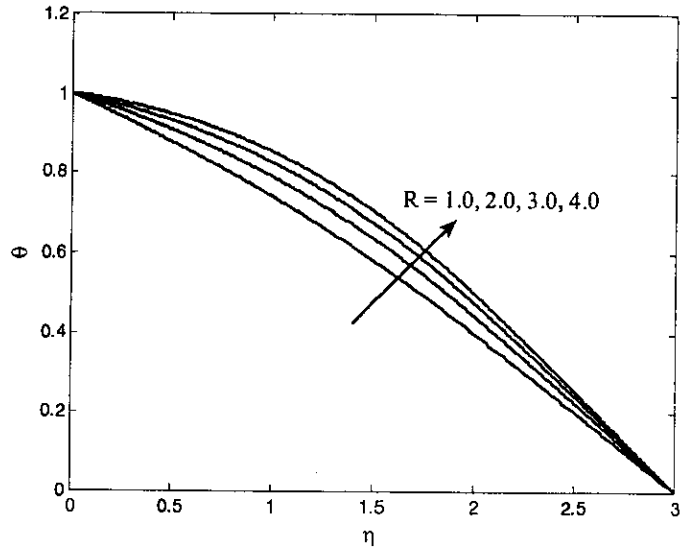

Figure 11: Temperature distribution for different R

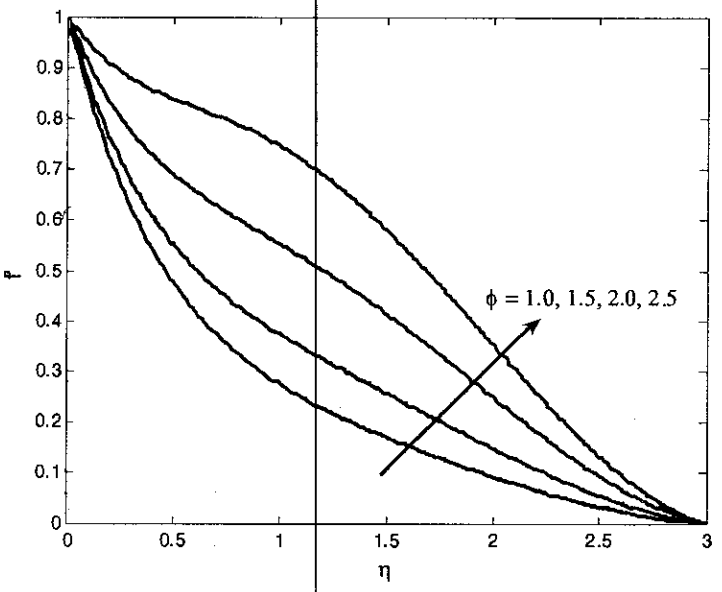

Figure 12: Velocity distribution for different ϕ

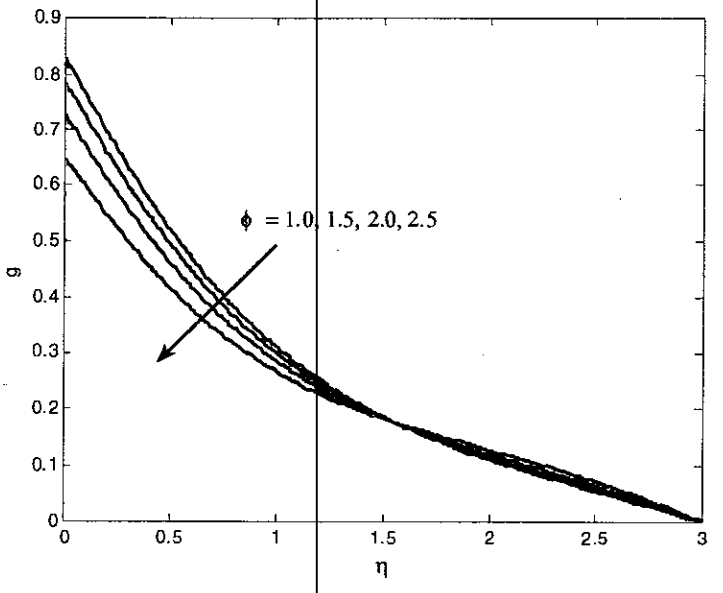

Figure 13: Microrotation distribution for different ϕ

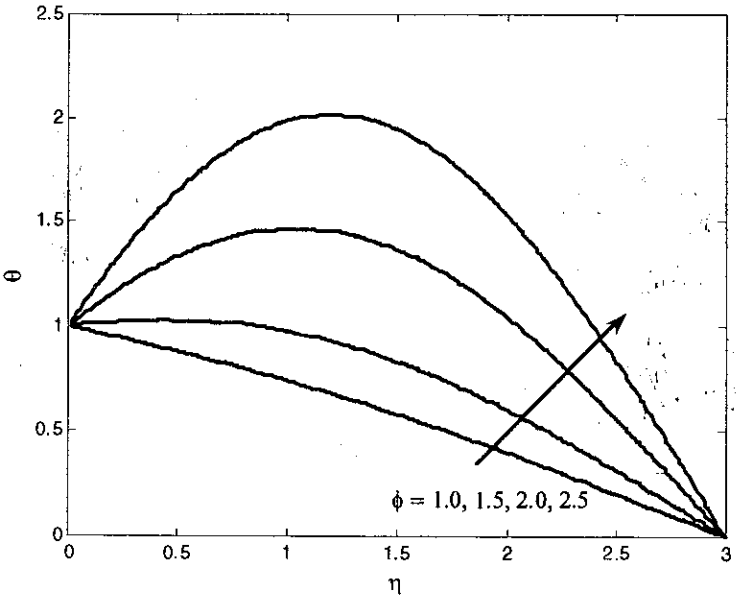

Figure 14: Temperature distribution for different ϕ

Table 1: Comparison of $-\theta'(0)$ for various values of M with $\phi = 0$

M	Raptis [7]	Present Work
0	0.355590	0.355581
1	0.384224	0.384238
2	0.397385	0.397391
3	0.4044361	0.404432

Table 2: Numerical values of the skin-friction coefficient and the Nusselt number for $\Pr = 0.71$.

Gr	K	M	ϕ	R	$f''(0)$	$-\theta'(0)$
1.0	1.0	1.0	1.0	1.0	0.925867	0.0647193
2.0	1.0	1.0	1.0	1.0	0.128817	0.126857
1.0	2.0	1.0	1.0	1.0	1.21334	0.0514129
1.0	1.0	2.0	1.0	1.0	1.42326	0.0430596
1.0	1.0	1.0	2.0	1.0	0.564008	1.11944
1.0	1.0	1.0	1.0	2.0	-0.66210	2.37658

REFERENCES

1. Eringen AC, (1966). "Theory of micropolar fluids", J. Math. Mech., 16, pp. 1–18.
2. R. S. R. Gorla, P. V. Reddy, Flow and Heat Transfer from a Continuous Surface in a Parallel Free Stream of Micropolar Fluid, *International Journal of Engineering Science*, Vol.25, No.10, 1987, pp. 1243-1249.
3. A. Raptis, Flow of a Micropolar Fluid past a Continuously Moving Plate by the Presence of Radiation, *International Journal of Heat and Mass Transfer*, Vol.41, No.18, 1998, pp. 2865- 2866.
4. H.A.M. El-Arabawy, Effect of suction/injection on the flow of a micropolar fluid past a continuously moving plate in he presence of radiation, *Int. J. Heat Mass Tran.*, 46, pp. 1471–1477, 2003.
5. M. A. Seddeek, S. N. Odda, M. Y. Akl, M. S. Abdelmeguid, Analytical solution for the effect of radiation on flow of a magneto-micropolar fluid past a continuously moving plate with suction and blowing, *Computational Materials Science*, Vol.45, No.2, pp. 423-42.
6. Brewster MQ (1992). *Thermal radiative transfer and properties*. John Wiley & Sons, New York.
7. A. Raptis, The flow of a micropolar fluid past a continuously moving plate by the presence of radiation. *International Journal of Heat and Mass Transfer* 41, 2865 (1998).